Energy Reports 8 (2022) 1853–1866

Contents lists available at ScienceDirect

Energy Reports

journal homepage: www.elsevier.com/locate/egyr

Research paper

A modified stochastic fractal search algorithm for parameter estimation of solar cells and PV modules

Shuhui Xu, Huadong Qiu *

School of Mechanical and Automotive Engineering, Qilu University of Technology (Shandong Academy of Sciences), Jinan, 250353, China
Shandong Institute of Mechanical Design and Research, Jinan, 250031, China

ARTICLE INFO

Article history:
Received 19 July 2021
Received in revised form 29 November 2021
Accepted 4 January 2022
Available online xxxx

Keywords:
Parameter estimation
Solar cell
Single diode model
Double diode model
Modified stochastic fractal search algorithm

ABSTRACT

In this work, a modified stochastic fractal search algorithm is proposed for effectively estimate the unknown model parameters of the single diode model and the double diode model of solar cells and photovoltaic modules. This algorithm modifies the diffusion process and the update processes of the original stochastic fractal search algorithm and employs a population size reduction mechanism and thus simplifies the implementation of the original algorithm and achieves better performance for the parameter estimation of solar cells and PV modules. Firstly, the algorithm is tested on three widely used estimation benchmark cases and compared with other seven state-of-the-art algorithms. The proposed algorithm shows its advantages in the aspects of accuracy, convergence speed, and stability over the other studied algorithms. In 100 independent runs with the maximum number of fitness function evaluations equal to 50000, the proposed algorithm achieved the best known solutions with 100% probability and the standard deviation of the 100 RMSE values is of the order of 10^{-17}. Then, the proposed algorithm is used to estimate the unknown single diode model parameters and double diode model parameters of three different types of PV modules, i.e. Multi-crystalline S75, Mono-crystalline SM55, and Thin-film ST40 under different irradiance and temperature conditions, and the algorithm also achieves sufficiently accurate models. The root mean square of the error (RMSE) values between the obtained models and the actual current data are of the order of 10^{-2} or 10^{-3}. In view of its effectiveness and practicability, the proposed algorithm can be used as a new tool for the parameter estimation of solar cells and PV modules.

1. Introduction

Confronted with the increasingly serious environmental and social problems caused by the extensive exploitation and utilization of traditional fossil energy, countries around the world are turning their attention to renewable energy (Ahmad et al., 2020; Mohamed et al., 2019). Among various renewable energy, solar energy is considered as one of the most promising as a result of its advantages such as abundant reserves, wide availability, cleanliness and so on (Chander et al., 2015; Kabir et al., 2018; Sansaniwal et al., 2018). The current utilization of solar energy mainly includes photoelectric conversion, photothermal conversion and photochemical conversion (Wang et al., 2019). Among them, photoelectric conversion is a kind of energy utilization approach which transfers sunshine into electricity directly using photovoltaic systems (Chander et al., 2015). Owing to its benefits such as safe, longevity of service, low maintenance cost, high cost effectiveness, and so on, photovoltaic systems have been rapidly developed all over the world (Kler et al., 2017; Muangkote et al., 2019; Taghezouit et al., 2021).

Solar cells and photovoltaic modules are important components of a photovoltaic system. It is of great significance to establish mathematical models to accurately describe their current–voltage (I–V) characteristics, because accurate models can help the designer to better understand the behavior of the cells and modules, so as to provide supports for the analysis, evaluation, optimization, maximum power point tracking, and fault diagnosis of the photovoltaic system (Jordehi, 2016; Kler et al., 2019). The electrical characteristics of a solar cell/module can be described using lumped parameter equivalent circuit models, and usually the single diode model (SDM) and the double diode model (DDM) are used (Xiong et al., 2018). SDM is made up of a current source, a diode, a parallel resistor, and a series resistor, and it achieves a good tradeoff between simplicity and accuracy. Compared with SDM, another diode in parallel with the first diode is added in DDM. DDM is more complex but more accurate than SDM, especially in low irradiation (Kler et al., 2019).

* Corresponding author at: School of Mechanical and Automotive Engineering, Qilu University of Technology (Shandong Academy of Sciences), Jinan, 250353, China.
E-mail address: qiuhuadong2021@126.com (H. Qiu).

https://doi.org/10.1016/j.egyr.2022.01.008

Nomenclature

D	dimension of the problem
DDM	double diode model
DSCSE	Metaphor-free dynamic spherical evolution
FEs	current number of fitness function evaluations
G	current number of iterations
Gauss(μ, δ)	Gaussian distribution with a mean of μ and a standard deviation of δ
GW_1	The first Gaussian random walk
IAE	absolute value of the difference
I_C	output current of the solar cell (A)
I_d	diode current (A)
IJAYA	improved JAYA algorithm
I_{ph}	photo generated current (A)
I_{sd}, I_{sd1}, I_{sd2}	reverse saturation current (μA)
I_{sh}	shunt resistor current (A)
P	the current population
P_{best}	the best one in solution population
PGJAYA	performance-guide JAYA algorithm
P_i	the ith solution in P
P_i'	trail solution generated by SFS for P_i
$\tilde{P}$	shuffled population based on P
$\hat{P}$	shuffled population based on P
P_{mean}	mean of all solutions in population
P_{r1}, P_{r2}	randomly selected solution
PSFS	perturbed stochastic fractal search
PSOCS	Random Reselection Particle Swarm Optimization
PV	photovoltaic
P-V	power vs. voltage
q	the charge of the electron ($1.60217646 \times 10^{-19}$ C)
I–V	current vs. voltage
k	Boltzmann constant (1.3806503×10^{23} J/K)
$L(j)$	lower bound of the jth design variable
Max_FEs	maximum number of fitness function evaluations
MDN	maximum diffusion number
MLBSA	multiple learning backtracking search algorithm
n, n_1, n_2	ideality factor
N_P	number of parallel cells
NP	population size
$NP_{initial}$	initial population size
NP_{final}	final population size
Ns	number of series cells
rand(0, 1)	random number uniformly distributed between [0, 1]
RMSE	root mean square of the error
γ_i	selection probability of SFS
R_s	the series resistance (Ω)
R_{sh}	shunt resistance (Ω)
SDM	single diode model
SFS	stochastic fractal search
T	temperature in Kelvin degree (K)
TLABC	teaching–learning–based artificial bee colony
$U(j)$	upper bound of the jth design variable
V_C	output voltage of the cell (V)

SDM and DDM respectively contains five and seven parameters and their values directly determine the accuracy of the model. Nevertheless, these values are not given in the datasheet of the solar cell or PV module and would change with the environmental conditions such as temperature and light intensity. Therefore, to determine the values of these parameters is a primary task in the modeling work.

According to the implementation principle, the method of determining model parameters can be classified as analytical methods and optimization methods (Kler et al., 2019; Xiong et al., 2021). Analytical methods use elementary functions to approximate explicit function expressions of the model parameters based on different degrees of assumptions and various simplified conditions, and then calculate the approximate value of each parameter by solving these function expressions simultaneously. Analytical methods have the advantages of simplicity and fast calculation speed, but when the model is complex and there are many unknown parameters, the set of equations that need to be established will increase, and the corresponding calculations will be more complicated. At the same time, analytical methods often require several specific points on the I–V characteristic curve. Unfortunately, these points may be not provide by PV manufacturers, especially when the cells or modules are working under non-standard test conditions. In addition, the simplifications and assumptions made in the solving process would also reduce the accuracy of model parameters (Jordehi, 2016; Kler et al., 2019; Merchaoui et al., 2018). Different from the analytical methods, optimization methods firstly transform the parameter identification problem of solar cells and modules into an optimization problem from the perspective of curve fitting, and then use optimization algorithms to obtain the model parameters which can make the model close to the real current and voltage data of photovoltaic cells and modules (Xiong et al., 2018). However, it is very challenging to obtain the optimal model parameters since the objective function is nonlinear, complex, implicit, multimodal, and transcendental (Chen et al., 2019; Zhang et al., 2020b). Therefore, the optimization algorithms used in the optimization methods should be very effective. The currently used optimization algorithms can be grouped into two categories: deterministic methods and meta-heuristic optimization algorithms (Zhang et al., 2020a). The deterministic methods are often designed based on some mathematical principles and belongs to the category of traditional optimization algorithms, and the disadvantage of these algorithms is that they often have very strict restrictions in application, such as requiring the objective function to be convex and differentiable. At the same time, these algorithms are usually skilled in local search, when being used to deal with the solar cell model parameter estimation problem, they are easy to fall into the local optimum. In addition, these algorithms are also very sensitive to the initial solution. If the initial solution is not appropriate, the final result will be very inferior (Kler et al., 2019; Xiong et al., 2021). Meta-heuristic algorithms have incomparable advantages over traditional algorithms in these aspects. Meta-heuristic algorithms treat the problem to be solved as a black box, and have no strict requirements on the mathematical properties of the objective function. Meanwhile, they are not sensitive to the initial

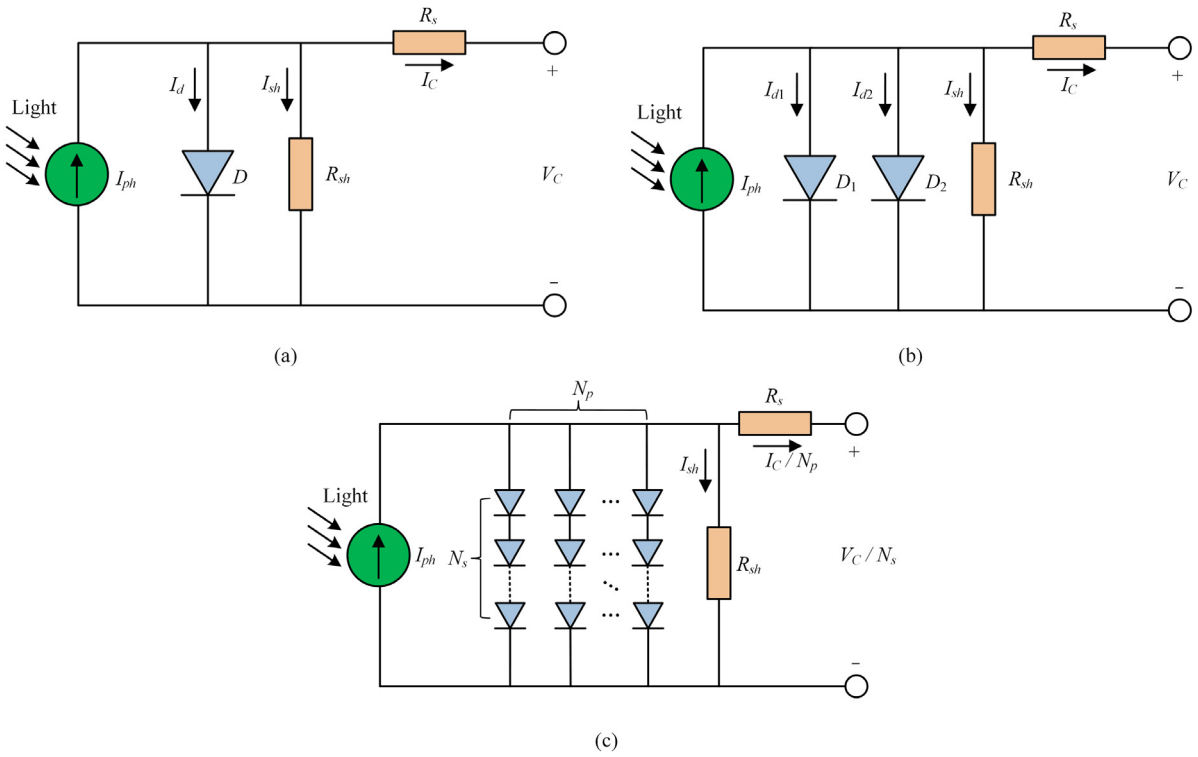

Fig. 1. (a) SDM of solar cell, (b) DDM of solar cell, (c) SDM of PV module.

value. In addition, the possibility of these algorithms falling into the local optimum can also be reduced by carefully designing the algorithms' operators (Kler et al., 2019; Liang et al., 2020). Therefore, meta-heuristic algorithms have attracted the attention of many researchers and many approaches for solving this problem based on different meta-heuristic algorithms are proposed, such as enhanced exploratory salp chains-based approach (Abbassi et al., 2020), orthogonally adapted Harris hawks optimization (Jiao et al., 2020), whippy Harris hawks optimization algorithm (Naeijian et al., 2021), reinforcement learning-based differential evolution (Hu et al., 2021), teaching–learning–based artificial bee colony (Chen et al., 2018), improved equilibrium optimizer algorithm (Wang et al., 2021a), Boosting slime mould algorithm (Liu et al., 2021a), perturbed stochastic fractal search (Chen et al., 2019), modified shuffling frog-leaping algorithm (Fan et al., 2021; Liu et al., 2021b; Wang et al., 2021b), Gradient-based optimization with ranking mechanisms (Ahmadianfar et al., 2021), performance-guided JAYA algorithm (Yu et al., 2019), flexible particle swarm optimization algorithm (Ebrahimi et al., 2019), Laplacian modified spherical evolution (Weng et al., 2021; Zhou et al., 2021), multiple learning backtracking search algorithm (Yu et al., 2018), boosted LSHADE algorithm (Ridha et al., 2021), Random reselection particle swarm optimization (Fan et al., 2022), and many others (Ben Messaoud, 2020; Jordehi, 2016; Mi et al., 2021). Though so many approaches have been proposed to deal with this problem, there is still a lot of room for improvement. Many researchers are devoting themselves to look for novel and effective approaches with smaller number of control parameters, faster convergence speed, greater ability to find more accurate solutions, and higher robustness.

In this study, a modified stochastic fractal search algorithm is proposed for solving this problem and its performance is verified using three parameter estimation cases and compared with several state-of-the-art approaches. It is found the proposed approach performs better in the terms of accuracy, convergence speed, and robustness.

The main contributions of this work can be summarized as follows:

(1) A modified stochastic fractal search algorithm, MSFS, is proposed for parameter estimating of the single diode model and the double diode model of solar cells and PV models.

(2) Compared with the original stochastic fractal search algorithm, MSFS has a simpler implementation process and better performance in photovoltaic model identification.

(3) Compared with seven state-of-the-art algorithms specifically designed for the parameter estimation problem of PV models, MSFS shows its advantages in the aspects of accuracy, convergence speed, and stability.

The rest of this paper is organized as follows. The mathematical description of the solar cell and PV module model parameter estimation problem is introduced in Section 2. The proposed modified stochastic fractal search algorithm is detailedly introduced in Section 3. The numerical experiments, results, and discussions are given in Section 4. The conclusions and possible further work are finally given in Section 5.

2. Problem description

Single diode model (SDM) and double diode model (DDM) are the core of the solar cell and PV module model parameter estimation problem, and the details of them are respectively given in below.

2.1. Single diode model

Fig. 1(a) is the circuit diagram of the SDM. According to the law of Kirchhoff, the output current of the solar cell I_C can be expressed as Eq. (1) (Chen et al., 2019; Yu et al., 2019):

$$I_C = I_{ph} - I_d - I_{sh} \tag{1}$$

where I_{ph}, I_d, and I_{sh} are respectively the photo generated current, the diode current, and the shunt resistor current. I_d and I_{sh} can be

respectively calculated as Eqs. (2) and (3).

$$I_d = I_{sd}\left[\exp\left(\frac{q\,(V_C + I_C R_s)}{nkT}\right) - 1\right] \tag{2}$$

$$I_{sh} = \frac{V_C + I_C R_s}{R_{sh}} \tag{3}$$

where I_{sd} and n respectively denote the reverse saturation current and the ideality factor of the diode, R_s and R_{sh} respectively denote the series resistance and the shunt resistance, V_C denotes the output voltage of the cell, k (1.3806503×10^{23} J/K) is the Boltzmann constant, T is the temperature of the junction in Kelvin degree, and q ($1.60217646 \times 10^{-19}$ C) is the elementary charge.

Based on Eqs. (1), (2), and (3), the following equation can be obtained. Totally, SDM contains five model parameters, i.e. I_{ph}, I_{sd}, R_s, R_{sh}, and n.

$$I_C = I_{ph} - I_{sd}\left[\exp\left(\frac{q\,(V_C + I_C R_s)}{nkT}\right) - 1\right] - \frac{V_C + I_C R_s}{R_{sh}} \tag{4}$$

2.2. Double diode model

Fig. 1(b) is the circuit diagram of the DDM. For the DDM, I_C can be formulated as Eq. (5) and as Eq. (6) in more detail (Chen et al., 2019; Yu et al., 2019). Accordingly, DDM totally contains seven model parameters, i.e. I_{ph}, I_{sd1}, I_{sd2}, R_s, R_{sh}, n_1, and n_2.

$$I_C = I_{ph} - I_{d1} - I_{d2} - I_{sh} \tag{5}$$

$$I_C = I_{ph} - I_{sd1}\left[\exp\left(\frac{q\,(V_C + I_C R_s)}{n_1 kT}\right) - 1\right] - I_{sd2}\left[\exp\left(\frac{q\,(V_C + I_C R_s)}{n_2 kT}\right) - 1\right] - \frac{V_C + I_C R_s}{R_{sh}} \tag{6}$$

2.3. PV module model

A typical PV module is made up of several same solar cells which are connected in parallel or in series. Fig. 1(c) shows its circuit diagram. For such a PV module, its output current I_C can be formulated as Eq. (7) based on the SDM (Chen et al., 2019; Yu et al., 2019).

$$I_C = N_p \cdot I_{ph} - N_p \cdot I_{sd}\left[\exp\left(\frac{q\left(V_C/N_s + I_C R_s/N_p\right)}{nkT}\right) - 1\right] - \frac{N_p \cdot V_C/N_s + I_C R_s}{R_{sh}} \tag{7}$$

where N_s and N_p are respectively the numbers of solar cells connected in series and in parallel.

2.4. Objective function

The purpose of the parameter estimation is to determine the optimal value of the model parameters, so as to make the model be consistent with the experimental data results as much as possible. From the point of view of optimization, an objective function that can reflect how well the model matches the experimental data is essential. Usually, the root mean square of the error (RMSE) as Eq. (8) is used (Jordehi, 2016; Yang et al., 2020).

$$\mathrm{RMSE}(X) = \sqrt{\frac{1}{N}\sum_{i=1}^{N} f(V_{Ci}, I_{Ci}, X)^2}, \tag{8}$$

where X denotes a candidate solution, i.e. a given set of model parameter values, N denotes the number of the experimental I–V data pairs.

Based on Eqs. (4), (6), and (7), the parameter estimation problem can be respectively formulated as follows.

For the SDM,

$$\begin{cases} \min f(V_C, I_C, X) = I_{ph} - I_{sd}\left[\exp\left(\dfrac{V_C + I_C R_s}{nV_t}\right) - 1\right] - \dfrac{V_C + I_C R_s}{R_{sh}} - I_C \\ X = \{I_{ph}, I_{sd}, R_s, R_{sh}, n\} \end{cases} \tag{9}$$

For the DDM,

$$\begin{cases} \min f(V_C, I_C, X) = I_{ph} - I_{sd1}\left[\exp\left(\dfrac{V_C + I_C R_s}{n_1 V_t}\right) - 1\right] - I_{sd2}\left[\exp\left(\dfrac{V_C + I_C R_s}{n_2 V_t}\right) - 1\right] - \dfrac{V_C + I_C R_s}{R_{sh}} - I_C \\ X = \{I_{ph}, I_{sd1}, I_{sd2}, R_s, R_{sh}, n_1, n_2\} \end{cases} \tag{10}$$

For the PV module model,

$$\begin{cases} \min f(V_C, I_C, X) = N_p \cdot I_{ph} - N_p \cdot I_{sd}\left[\exp\left(\dfrac{V_C/N_s + I_C R_s/N_p}{nV_t}\right) - 1\right] - \dfrac{N_p \cdot V_C/N_s + I_C R_s}{R_{sh}} - I_C \\ X = \{I_{ph}, I_{sd}, R_s, R_{sh}, n\} \end{cases} \tag{11}$$

3. The proposed method

3.1. Original stochastic fractal search

As a population-based meta-heuristic algorithm, stochastic fractal search (SFS) mimics the natural phenomenon of growth (Salimi, 2015). It contains two main processes named diffusion and updating respectively. The former attempts to find a better solution for every solution around its current location by Gaussian random walks and is considered as the exploitation phase, and the latter is considered as the exploration phase and in this process, the attempt solution for every current solution is generated according to the location of other solutions in current population.

In the diffusion process, a predetermined parameter called maximum diffusion number (MDN) is used to control the number of attempts for each current solution. In other words, MDN trial solutions would be generated for each solution. If the best one of them is superior to the current solution, the current solution would be displaced by it, or else, the current solution would not be changed. In original SFS, two kinds of Gaussian random walks are defined for generating the trial solutions. The second Gaussian random walk would not be introduced here because it is not used in this study, while the first one is described as Eq. (12) (Salimi, 2015).

$$GW_1 = \mathrm{Gaussian}\,(\mu_{BP}, \delta) + (\mathrm{rand}(0, 1) \times P_{\mathrm{best}} - \mathrm{rand}(0, 1) \times P_i) \tag{12}$$

where Gaussian (μ, δ) denotes the Gaussian distribution with a mean of μ and a standard deviation of δ, rand(0, 1) is a random number which is uniformly distributed between [0, 1], P_{best} and P_i are respectively the best solution and the ith solution in current population. μ_{BP} and μ_P are equal to P_{best} and P_i, respectively, δ dynamically changes with the number of the iterations, as shown

in Eq. (13) (Salimi, 2015), where G denotes the current number of iterations.

$$\delta = \left| \frac{\log(G)}{G} \times (P_i - P_{\text{best}}) \right| \tag{13}$$

The updating process of SFS can be further divided into two phases. In the first phase, all the solutions in current population are ranked based on their quality from the best to the worst and then assigned a selection probability γ_i, which is calculated according to Eq. (14) (Salimi, 2015), where rank(P_i) is the order of the ith solution in the population. Then, SFS would generate a trial solution P_i' for each solution P_i according to Eq. (15) (Salimi, 2015), where D is the dimension of the optimization problem $j \in \{1, 2, \ldots, D\}$ is the index of each design variable, $\tilde{P}$ and $\hat{P}$ denotes two populations obtained by randomly shuffling the order of the solutions in P, as described by Eq. (16) (Salimi, 2015), where permuting is a random shuffling function. If P_i' is better than P_i, then P_i would be replaced by P_i'.

$$\gamma_i = 1 - \frac{rank(P_i)}{NP} \tag{14}$$

$$P_i'(j) = \begin{cases} \tilde{P}_i(j) - \text{rand}(0, 1) \times \left(\hat{P}_i(j) - P_i(j) \right) & \text{if } \gamma_i < \text{rand}(0, 1) \\ P_i(j) & \text{otherwise} \end{cases} \tag{15}$$

$$\begin{cases} \tilde{P} = \text{permuting}(P) \\ \hat{P} = \text{permuting}(P) \end{cases} \tag{16}$$

In the second phase, the probability γ_i would be recalculated, and for each solution P_i, SFS would produce a trail solution P_i' according to Eq. (17) (Salimi, 2015) with a probability of γ_i, where P_{r1} and P_{r2} are two different solutions randomly selected from the population. Similarly with the first phase, if the newly-generated trial solution is better than P_i, then P_i would be replaced by it.

$$P_i' = \begin{cases} P_i - \text{rand}_1(0, 1) \times (P_{r1} - P_{\text{best}}), & \text{if } \text{rand}_2(0, 1) \le 0.5 \\ P_i + \text{rand}_1(0, 1) \times (P_{r1} - P_{r2}), & \text{otherwise} \end{cases} \tag{17}$$

Limited by the length of this article, only a brief introduction about the operators of SFS is given here, more details about SFS can be found in Salimi (2015).

3.2. Modifications on the diffusion process

In this work, some modifications are made to better balance the exploitation and exploration. The first modification we made to the original SFS is on the diffusion process. The original operators in the diffusion process are replaced by Eq. (18), where P_{mean} is the mean of all solutions in the current population, and it is calculated according to Eq. (19), where NP denotes the population size. This modification is inspired by the famous bare-bones particle swarm optimization (Kennedy, 2003; Pan et al., 2008).

$$P_i'(j) = \text{Gaussian}\left(P_{mean}(j), |P_{mean}(j) - P(j)|\right) \tag{18}$$

$$P_{mean}(j) = \frac{1}{NP} \sum_{i=1}^{NP} P_i(j) \tag{19}$$

3.3. Modifications on the update processes

Some modifications are also made on the update processes. Firstly, both in the first updating process and the second updating process, the selection probability described by Eq. (14) is removed. Accordingly, Eq. (15) is replaced by Eq. (20). Furthermore, an additional condition, $r_1 \neq r_2 \neq i$, is added to Eq. (17).

$$P_i'(j) = \tilde{P}_i(j) - \text{rand}(0, 1) \times \left(\hat{P}_i(j) - P_i(j) \right) \tag{20}$$

In the modified update processes, the operators denoted by Eqs. (20) and (17) are carried out on every solution in the current population, rather than being carried out with a calculated probability.

3.4. Population size reduction strategy

Population size is functionally important in the performance of a meta-heuristic algorithm (Fernandes et al., 2020; Piotrowski et al., 2020; Poláková et al., 2019). At the early stage of the solving process, a large population is beneficial to maintain the diversity of the population and help the algorithm to find good-quality solutions, while at the latter stage, a large population may result in a waste of computational resources because the differences between the solutions are very small at this stage. For this situation, appropriately reducing the population size during the solving process is conducive to saving computing resources. This point has been proven by many previous studies (Brest and Maučec, 2011; Brest et al., 2017; Brest and Sepesy Maučec, 2008; Tanabe and Fukunaga, 2014). Inspired by this, a population size reduction strategy is designed in the modified SFS. In detail, in every generation, the population size NP_G would be calculated according to Eq. (21), where $NP_{initial}$ and NP_{final} respectively denote the initial population size and the final population size, FEs and Max_FEs respectively denote the current number of and the maximum number of fitness function evaluations, round[·] denotes the rounding-off rule. If the current population size is larger than NP_G, only the best NP_G solutions in current population would be retained and the others would be directly discarded.

$$NP_G = \text{round}\left[NP_{initial} - \frac{FEs}{Max\_FEs} * (NP_{initial} - NP_{final}) \right] \tag{21}$$

3.5. Bound constraint-handling method

In the solving process of a meta-heuristic algorithm, new solutions may be generated outside the search space. These solutions should be fixed using some bound constraint-handling methods in time, otherwise the efficiency of the algorithm may be reduced, or even wrong results may be obtained. Many different bound constraint-handling methods have been proposed, and different methods may lead to different performances (Chu et al., 2011; Gandomi and Yang, 2012). In the modified SFS, a simple bound constraint-handling method is adopted, as shown in Eq. (22), where $P(j)$ denotes the value of the jth variable in solution P, and $L(j)$ and $U(j)$ respectively denote the lower bound and the upper bound of the jth design variable.

$$\begin{aligned} &P(j) = L(j) + \text{rand}(0, 1) \times (U(j) - L(j)) \\ &\text{if } P(j) < L(j) \text{ or } P(j) > U(j) \end{aligned} \tag{22}$$

3.6. The proposed modified SFS

The modified stochastic fractal search algorithm is proposed based on the modifications above. Fig. 2 gives its pseudo-code, from where it can be found that the modified SFS is very easy to implement due to its simple structure.

The modified stochastic fractal search algorithm

Set the search ranges (up boundary UB and low boundary LB), the initial population size $NP_{initial}$, the final population size NP_{final}, and the end condition Max_FEs;
Randomly generated a solution population with $NP_{initial}$ solutions;
Evaluate the fitness function value for every initial solution;
$FEs=NP_{initial}$;
while $FEs < Max\_NFFEs$
  //Diffusion process
  Caculate the mean of current population according to Eq.(19);
  for $i = 1 : NP_G$
    Generate a trial solution P_i according to Eq.(18) and limit it in the search space using Eq.(22);
    Evaluate the fitness function value of P_i;
    $FEs = FEs+1$;
    if P_i is better than P_i, **then**
      Replace P_i by P_i;
    end if
  end for
  //First updating process
  Obtain $\tilde{P}$ and $\hat{P}$ using Eq.(16);
  for $i = 1 : NP_G$
    Generate a trial solution P_i' according to Eq.(20) and limit it in the search space using Eq.(22);
    Evaluate the fitness function value of P_i';
    $FEs = FEs+1$;
    if P_i' is better than P_i, **then**
      Replace P_i by P_i';
    end if
  end for
  //Second updating process
  Determine the best solution in current population P_{best};
  for $i = 1 : NP_G$
    Randomly selected two integers r_1 and r_2 from 1 to NP_G, which satisfy $r_1 \neq r_2 \neq i$;
    Generate a trial solution P_i' according to Eq.(17) and limit it in the search space using Eq.(22);
    Evaluate the fitness function value of P_i';
    $FEs = FEs+1$;
    if P_i' is better than P_i, **then**
      Replace P_i by P_i';
    end if
  end for
  //Reduce the population size
  Caculate the population size NP_G for next generation according to Eq.(21), and only retain the best NP_G solutions in the population.
end while

Fig. 2. The pseudo-code of the proposed MSFS algorithm.

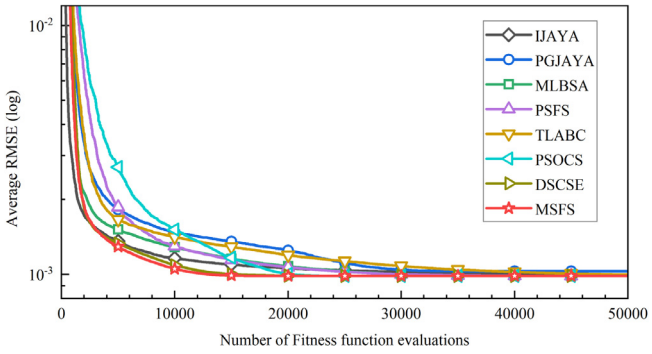

Fig. 3. The average convergence curves of the tested algorithms on the first case.

4. Experimental results and discussions

To verify its performance, the modified SFS (MSFS) is firstly examined on three widely-used benchmark parameters estimation cases borrowed from literature (Easwarakhanthan et al., 1986). The first two cases aim to estimate the SDM parameters and the DDM parameters of a commercial RTC France silicon solar cell which works at the environmental temperature of 33 °C and the environmental irradiance of 1000 W/m^2, and the third case aims to estimate the SDM parameters of a Photo watt-PWP 201 PV module consisting of 36 polycrystalline silicon cells connected in series which works at the environmental temperature of 45 °C and the environmental irradiance of 1000 W/m^2. Meanwhile, to demonstrate the competitiveness of MSFS, seven recent approaches designed for the parameter estimation of solar cell and PV module, including the improved JAYA algorithm (IJAYA) (Yu et al., 2017), the performance-guide JAYA algorithm (PGJAYA) (Yu et al., 2019), the multiple learning backtracking search algorithm (MLBSA) (Yu et al., 2018), the perturbed stochastic fractal search (PSFS) (Chen et al., 2019), the teaching–learning–based artificial bee colony (TLABC) (Chen et al., 2018), the Random Reselection Particle Swarm Optimization (PSOCS) (Fan et al., 2022), and the Metaphor-free dynamic spherical evolution (DSCSE) (Zhou et al., 2021) are also tested in this work for comparison. Then, to further examine its practicability, the proposed algorithm is used to estimate the SDM parameters and DDM parameters of three

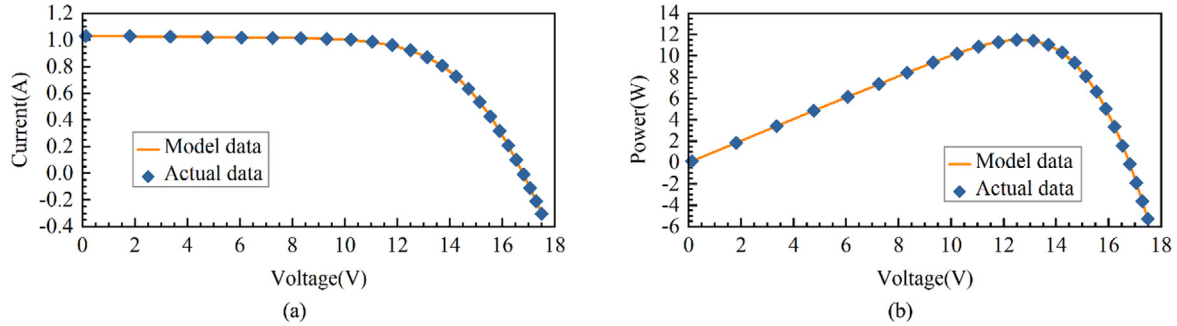

Fig. 4. Consistency between the estimated SDM and the actual solar cell (a) *I–V* characteristic, (b) *P-V* characteristic.

Table 1
Lower bound and upper bound of each model parameter.

Model parameter	RTC France silicon solar cell		Photo watt-PWP 201 PV module	
	Lower bound	Upper bound	Lower bound	Upper bound
I_{ph} (A)	0	1	0	2
I_{sd} (μA)	0	1	0	50
R_{sh} (Ω)	0	100	0	2000
R_s (Ω)	0	0.5	0	2
n	1	2	1	50

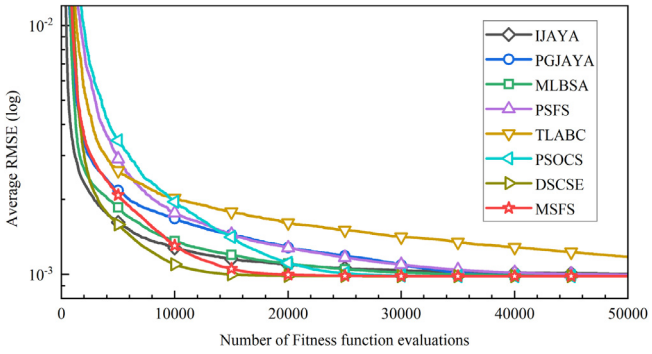

Fig. 5. The average convergence curves of the tested algorithms on the second case.

different types of solar modules, i.e. Multi-crystalline S75, Mono-crystalline SM55, and Thin-film ST40 under different irradiance and temperature conditions.

The experiments are carried out using MATLAB R2016b. The search ranges of model parameters for RTC France silicon solar cell and Photo watt-PWP 201 PV module are given in Table 1. The search ranges of model parameters for Multi-crystalline S75, Mono-crystalline SM55, and Thin-film ST40 are set as same as literature (Xu and Wang, 2017). The parameter values of each tested algorithm are given in Table 2, according to the suggestions given in the corresponding references. For every case, each algorithm is independently run 100 times to eliminate the effect caused by the randomness of the algorithms. Every run is ended when the maximum number of function evaluations (*Max_FEs*) reaches 50,000.

4.1. SDM on RTC France silicon solar cell data set

The RMSE results of all the tested algorithms on this case are statistically arranged in Table 3, where the best RMSE results are marked in boldface, to compare the performance differences of each algorithm in identification accuracy and stability. It can be observed that PSOCS, DSCSE and MSFS perform better than the others. All these three algorithms obtained the known optimal result (RMSE = 9.860219E−04) with 100% probability. Though there are other algorithms such as PGJAYA, MLBSA, and PSFS also achieved the known optimal result, PSOCS, DSCSE, and MSFS win out in stability. Furthermore, the performances of these three algorithms on this case are similar because the standard deviations of their results are very close. IJAYA and TLABC performed worse because they failed to achieve the known optimal result. The best model parameters obtained by each algorithm are given in Table 4. From which it can be found that the best parameters obtained by different algorithms are very close. This indicates that there are many locally optimal solutions in the neighborhood of the optimal solution.

The average convergence curves of these algorithms are given in Fig. 3. From this figure, it can be found that the convergence curves of DSCSE and MSFS are almost coincident. In other words, MSFS and DSCSE perform similarly in convergence rate. Furthermore, the obvious superiority of MSFS on convergence rate than the others can be observed. At the early stage of solving (*FEs* < 10,000), though the convergence curves of every algorithm decline quickly, the curve of MSFS decline more quickly than the others. After about 6000 fitness function evaluations, the convergence curve of MSFS starts to get ahead of the others and keeps this advantage until the solving process ends.

The *I–V* and *P-V* (power vs. voltage) characteristics of the solar cell and the SDM reconstructed using the best parameter values obtained by MSFS are given in Fig. 4. Meanwhile, the detail *I–V* data are arranged in Table A.1, where IAE is defined as the absolute value of the difference between the measured and the simulated current values. From Fig. 4 and Table A.1, the high agreement of the model and the measured data can be observed. At each measured voltage point, the difference between the measured current and the output current of the estimated SDM is very small. The maximum value of IAE is 2.5074E−03.

4.2. DDM on RTC France silicon solar cell data set

The RMSE results obtained by the tested eight algorithms for this case are statistically tabulated as Table 5, from where the better performance of MSFS can be concluded. Firstly, PSOCS,

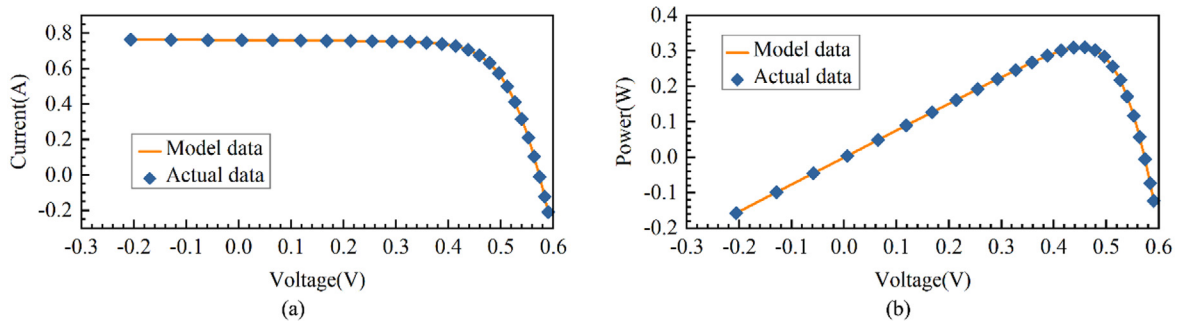

Fig. 6. Consistency between the estimated DDM and the actual solar cell (a) *I–V* characteristic, (b) *P-V* characteristic.

Table 2
The parameters of every algorithm used in this study.

Algorithm	Parameter values
IJAYA	$NP = 20$.
PGJAYA	$NP = 20$.
MLBSA	$NP = 50$.
PSFS	$NP = 30$, MDN $= 1$, Gaussian walk GW_1.
TLABC	$NP = 50$, $limit = 200$, $F =$ rand(0, 1).
DSCSE	$NP = 30$.
PSOCS	$NP = 30$, Pa $= 0.25$, $c_1 = c_2 = 2$, $V_{\max} = 6$; $w = 0.9–0.7^*(FEs/Max\_FEs)$.
MSFS	$NP_{initial} = 30$, $NP_{final} = 10$.

Table 3
Statistical comparison of RMSE values achieved by the tested algorithms for the first case.

Algorithm	Min	Mean	Median	Max	Std
IJAYA	9.860328e−04	9.955406e−04	9.883849e−04	1.438520e−03	4.551651e−05
PGJAYA	**9.860219e−04**	1.030240e−03	9.860222e−04	2.448049e−03	2.506042e−04
MLBSA	**9.860219e−04**	**9.860219e−04**	**9.860219e−04**	9.860231e−04	1.584194e−10
PSFS	**9.860219e−04**	9.860465e−04	**9.860219e−04**	9.869154e−04	1.189995e−07
TLABC	9.860222e−04	9.983721e−04	9.906584e−04	1.082772e−03	1.809366e−05
PSOCE	**9.860219e−04**	**9.860219e−04**	**9.860219e−04**	**9.860219e−04**	**3.037151e−17**
DSCSE	**9.860219e−04**	**9.860219e−04**	**9.860219e−04**	**9.860219e−04**	**6.097896e−17**
MSFS	**9.860219e−04**	**9.860219e−04**	**9.860219e−04**	**9.860219e−04**	**4.226479e−17**

Table 4
The best SDM parameter values achieved by the tested algorithms for the first case.

Parameter	IJAYA	PGJAYA	MLBSA	PSFS	TLABC	PSOCS	DSCSE	MSFS
I_{ph} (A)	0.76077573	0.76077553	0.76077553	0.76077553	0.76077547	0.76077553	0.76077553	0.76077553
I_{sd} (μA)	0.32262458	0.32302106	0.32302079	0.32302078	0.32311401	0.32302080	0.32302079	0.32302082
R_s (Ω)	0.03638051	0.03637709	0.03637709	0.03637709	0.03637591	0.03637709	0.03637709	0.03637709
R_{sh} (Ω)	53.69132921	53.71847623	53.71852350	53.71851884	53.73032623	53.71852340	53.71852102	53.71852461
n	1.48105920	1.48118367	1.48118359	1.48118358	1.48121255	1.48118359	1.48118358	1.48118359
RMSE	9.860328e−04	**9.860219e−04**	**9.860219e−04**	**9.860219e−04**	9.860222e−04	9.860219e−04	9.860219e−04	**9.860219e−04**

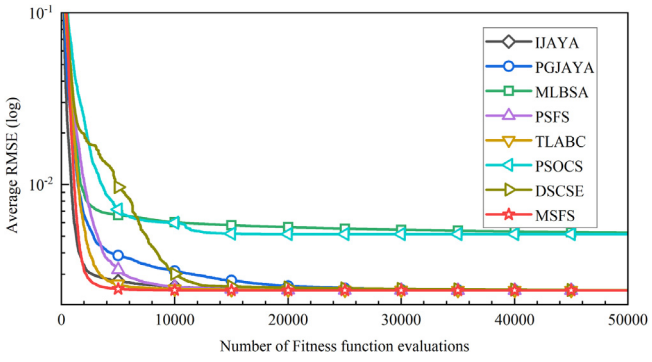

Fig. 7. The average convergence curves of the tested algorithms on the third case.

DSCSE, and MSFS succeeded in obtaining the known optimal solution of this case (RMSE = 9.824849e−04) while the others failed. Any reduction in RMSE value is still of great significance because there is no prior knowledge of the exact values of the model parameters. Therefore, it can be concluded that PSOCS, DSCSE and MSFS perform better than the others. Among PSOCS, DSCSE, and MSFS, it can be observed that MSFS wins the comparisons of the mean value and the maximum value of the RMSE values of the results they obtained. Furthermore, if we take the results obtained by MSFS with those obtained by it on the previous case, it can be found the min of RMSE values obtained on this case is smaller while the max of and the standard deviation of RMSE values obtained on this case are bigger. This demonstrates that compared with SDM, DDM can indeed describe the characteristics of the solar cell more precisely, on the other hand, the parameter estimation work for DDM is harder because DDM contains two more unknown parameters than SDM.

The average convergence curves of these algorithms on this case are given in Fig. 5, from which the obvious superiority of MSFS on convergence rate than the other algorithms can also be observed. At the stage of *FEs* < 10,000, MSFS lags behind IJAYA, MLBSA, and DSCSE, but after about 12,000 fitness function

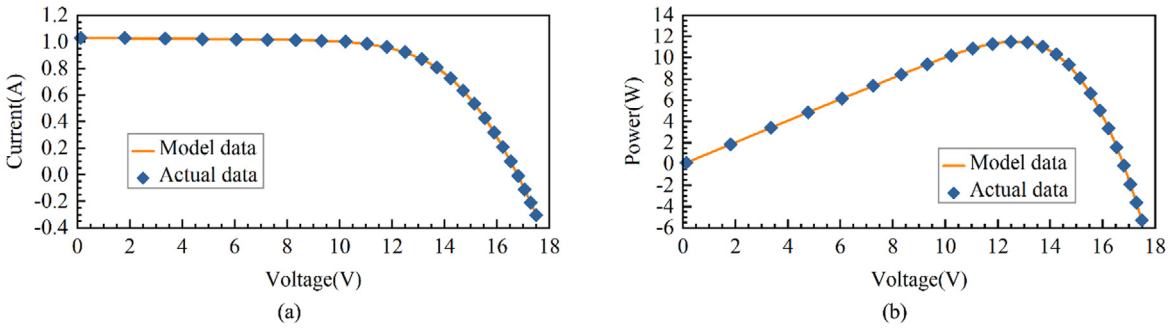

Fig. 8. Consistency between the estimated SDM and the actual PV module (a) *I–V* characteristic, (b) *P-V* characteristic.

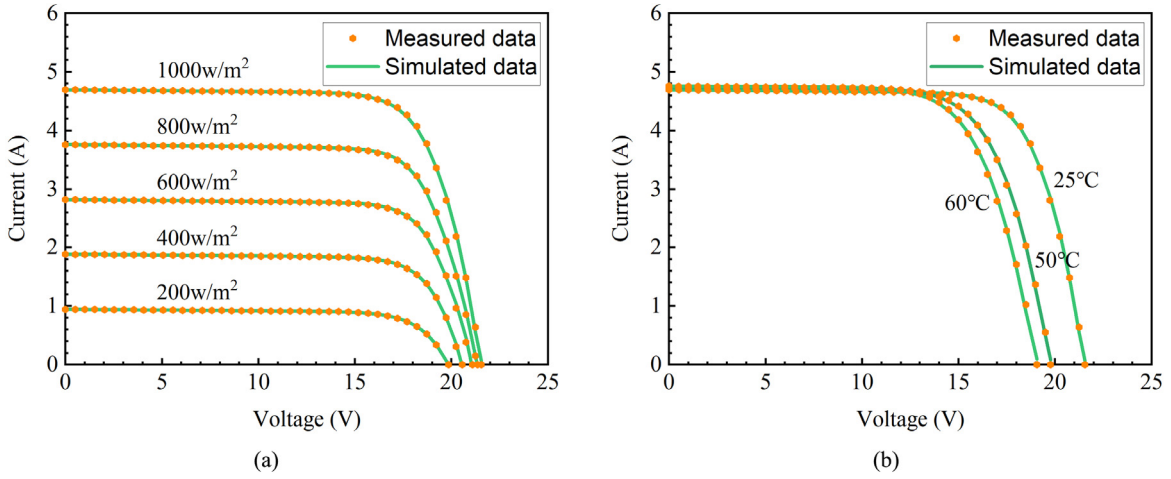

Fig. 9. Consistency between the *I–V* characteristics of the estimated SDM and the actual S75 module (a) different irradiances; (b) different temperatures.

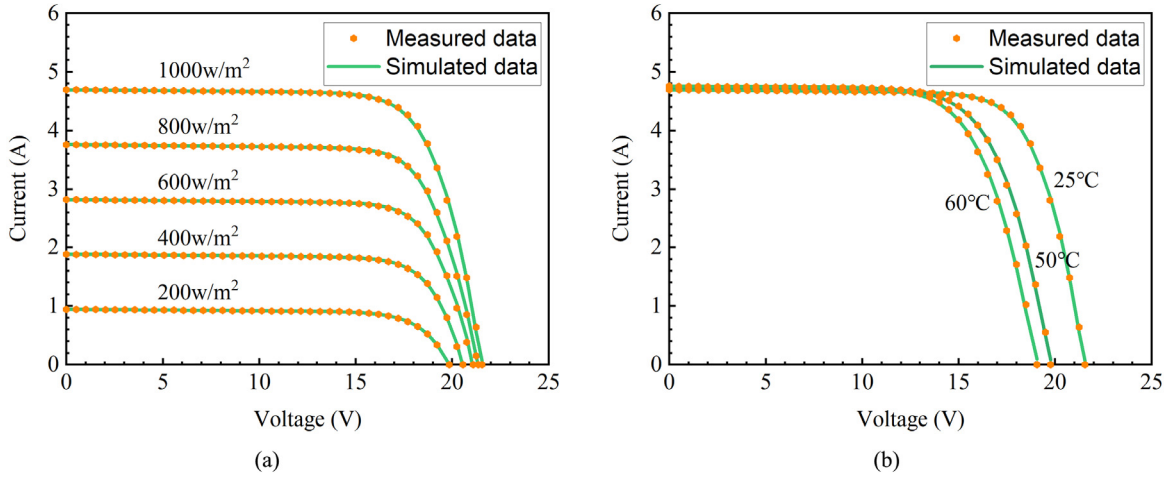

Fig. 10. Consistency between the *I–V* characteristics of the estimated DDM and the actual S75 module (a) different irradiances; (b) different temperatures.

evaluations, the convergence curve of MSFS is always ahead of the curves of the others except DSCSE. In consideration of all the solutions obtained by these algorithms at the early stage of the solving process are inferior, the advantage of MSFS shown in the middle and later stage of the solving process is more valuable.

The best model parameters obtained by each algorithm are given in Table 6. Based on these data, It can also be inferred that there are many locally optimal solutions in the neighborhood of the optimal solution of this case. The consistency between the best DDM obtained by MSFS and the actual behavior of the cell is illustrated using Fig. 6, and the detail data are given in Table A.1. It can be observed that the obtained DDM coincides with the experimental data very well. At each data point, the difference between the output current of the model and the actual current is very slightly. The maximum value of IAE is 2.5434E−03.

4.3. SDM on photo watt-PWP 201 PV module data set

The RMSE results obtained by the tested algorithms for this case are statistically tabulated as Table 7. Similar to the previous two cases, for this case, MSFS also gets better results than the others. Though the best RMSE values achieved by PGJAYA, MLBSA,

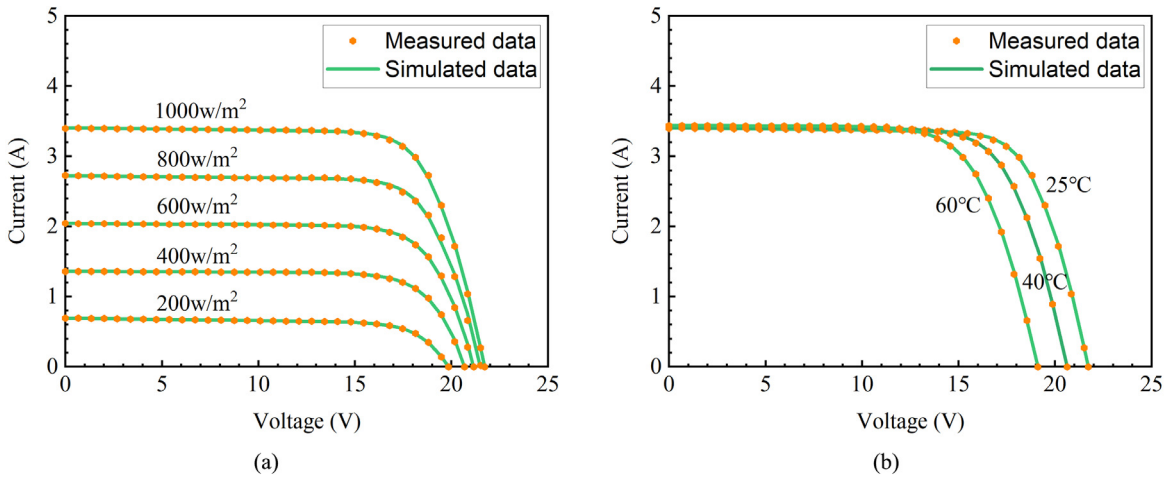

Fig. 11. Consistency between the *I*–*V* characteristics of the estimated SDM and the actual SM55 module (a) different irradiances; (b) different temperatures.

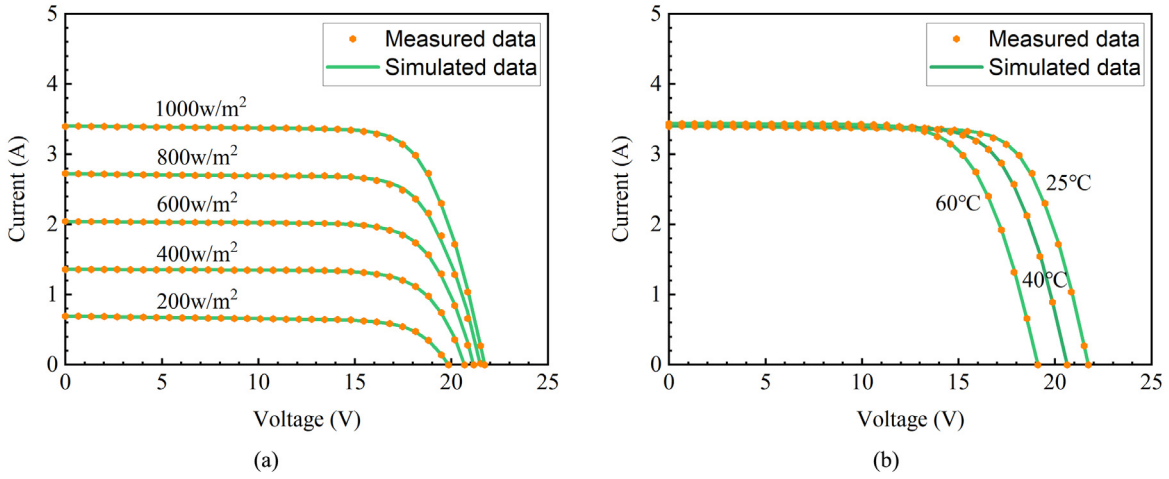

Fig. 12. Consistency between the *I*–*V* characteristics of the estimated DDM and the actual SM55 module (a) different irradiances; (b) different temperatures.

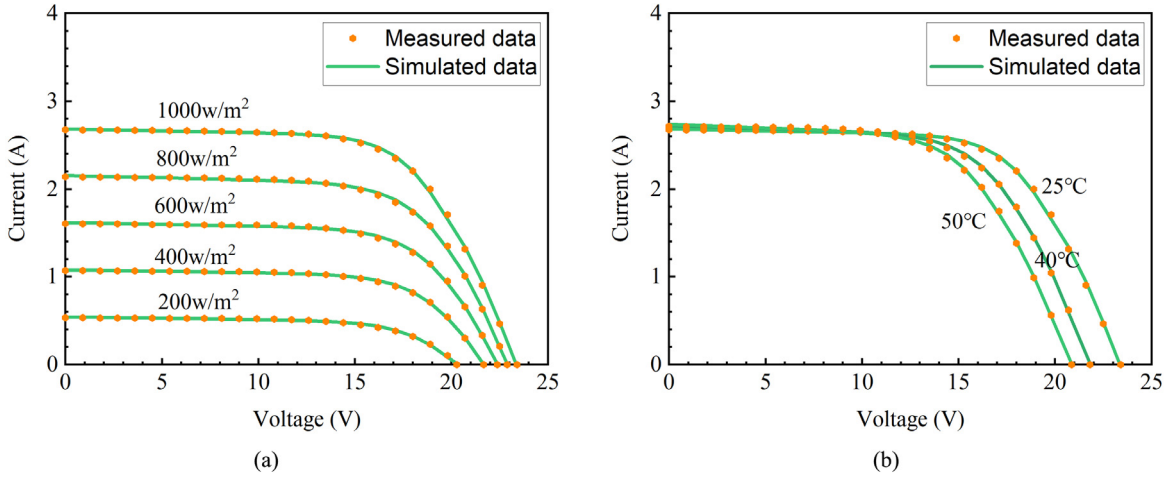

Fig. 13. Consistency between the *I*–*V* characteristics of the estimated SDM and the actual ST40 module (a) different irradiances; (b) different temperatures.

PSFS, TLABC, PSOCS, DSCSE, and MSFS are equal, MSFS wins out with better stability. The standard deviation of the RMSE values achieved by MSFS in the 100 experiments is only 3.531028e−17. In other words, the results obtained by MSFS in repeated independent experiments were little changed. Furthermore, compared with the first case, though this case is also based on SDM and contains five unknown model parameters, the search space is bigger and therefore the estimation task is harder. In this case, an algorithm may not perform as well as it performs in the first case, such as MLBSA, PSOCS, and DSCSE. In fact, our experiments shows that in this case, these three algorithms would fall into local

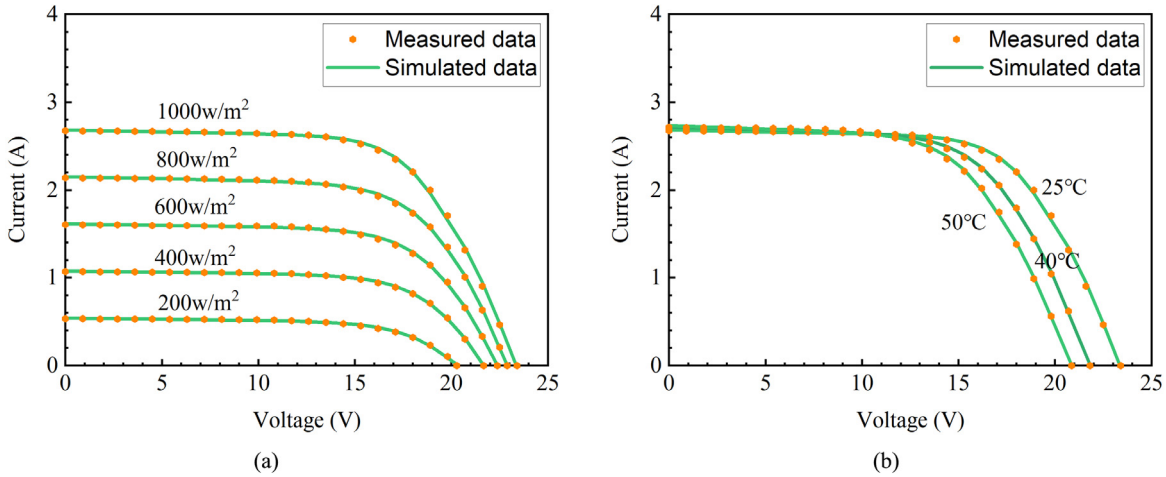

Fig. 14. Consistency between the *I–V* characteristics of the estimated DDM and the actual ST40 module (a) different irradiances; (b) different temperatures.

Table 5
Statistical comparison of RMSE values achieved by the tested algorithms for the second case.

Algorithm	Min	Mean	Median	Max	Std
IJAYA	9.849257e−04	1.005867e−03	9.926323e−04	1.437695e−03	5.882340e−05
PGJAYA	9.827438e−04	9.902110e−04	9.860259e−04	1.088853e−03	1.639368e−05
MLBSA	9.824881e−04	9.863995e−04	9.857497e−04	1.049833e−03	7.939137e−06
PSFS	9.824906e−04	9.971315e−04	9.859206e−04	1.324327e−03	4.422911e−05
TLABC	9.833842e−04	1.177675e−03	1.108683e−03	1.937772e−03	1.885548e−04
PSOCS	**9.824849e−04**	9.840464e−04	9.833830e−04	9.939448e−04	1.813929e−06
DSCSE	**9.824849e−04**	9.843049e−04	**9.833580e−04**	9.998500e−04	2.257666e−06
MSFS	**9.824849e−04**	**9.839962e−04**	9.834697e−04	**9.860519e−04**	**1.366613e−06**

Table 6
The best DDM parameter values achieved by the tested algorithms for the second case.

Parameter	IJAYA	PGJAYA	MLBSA	PSFS	TLABC	PSOCS	DSCSE	MSFS
I_{ph} (A)	0.76076852	0.76077781	0.76078027	0.76077858	0.76077702	0.76078108	0.76078108	0.76078108
I_{sd1} (μA)	0.27966751	0.24893659	0.72866923	0.22834960	0.24853873	0.22597442	0.74934889	0.74934896
R_s (Ω)	0.03648446	0.03663949	0.03672898	0.03672710	0.03660488	0.03674043	0.03674043	0.03674043
R_{sh} (Ω)	54.53408709	55.03511201	55.44307004	55.48371575	55.13211006	55.48543296	55.48544492	55.48543892
n_1	1.46954882	1.45912209	1.99999997	1.45190073	1.45944541	1.45101682	2.00000000	2.00000000
I_{sd2} (μA)	0.21264451	0.55829919	0.22841699	0.73050521	0.46978847	0.74934600	0.22597409	0.22597404
n_2	1.88870911	2.00000000	1.45191563	1.99994793	1.94839986	2.00000000	1.45101670	1.45101668
RMSE	9.849257e−04	9.827438e−04	9.824881e−04	9.824906e−04	9.833842e−04	**9.824849e−04**	**9.824849e−04**	**9.824849e−04**

Table 7
Statistical comparison of RMSE values achieved by the tested algorithms for the third case.

Algorithm	Min	Mean	Median	Max	Std
IJAYA	2.425080e−03	2.428477e−03	2.427160e−03	2.448762e−03	4.309266e−06
PGJAYA	**2.425075e−03**	2.425233e−03	2.425082e−03	2.429696e−03	5.558237e−07
MLBSA	**2.425075e−03**	5.249078e−03	**2.425075e−03**	2.742508e−01	2.718543e−02
PSFS	**2.425075e−03**	2.425312e−03	**2.425075e−03**	2.440176e−03	1.702666e−06
TLABC	**2.425075e−03**	2.425553e−03	2.425106e−03	2.432146e−03	1.206281e−06
PSOCS	**2.425075e−03**	5.146993e−03	**2.425075e−03**	2.742508e−01	2.718221e−02
DSCSE	**2.425075e−03**	2.427962e−03	**2.425075e−03**	2.713797e−03	2.887222e−05
MSFS	**2.425075e−03**	**2.425075e−03**	**2.425075e−03**	**2.425075e−03**	**3.531028e−17**

Table 8
The best SDM parameter values achieved by the tested algorithms for the third case.

Parameter	IJAYA	PGJAYA	MLBSA	PSFS	TLABC	PSOCS	DSCSE	MSFS
I_{ph} (A)	1.03052792	1.03051434	1.03051430	1.03051430	1.03051405	1.03051430	1.03051430	1.03051430
I_{sd} (μA)	3.47770893	3.48221224	3.48226330	3.48226296	3.48231813	3.48226286	3.48226311	3.48226280
R_s (Ω)	1.20140958	1.20127246	1.20127100	1.20127101	1.20127150	1.20127101	1.20127101	1.20127101
R_{sh} (Ω)	980.41458185	981.96900365	981.98242385	981.98232078	982.03936751	981.98227887	981.98237079	981.98218498
n	48.63781002	48.64277917	48.64283529	48.64283491	48.64289351	48.64283480	48.64283508	48.64283474
RMSE	2.425080e−03	**2.425075e−03**	**2.425075e−03**	**2.425075e−03**	**2.425075e−03**	**2.425075e−03**	**2.425075e−03**	**2.425075e−03**

optimum with very low probabilities. Therefore, the performance of MSFS on this case proves its competitiveness.

The average convergence processes of these algorithms on this case are compared in Fig. 7. The advantage of MSFS in convergence speed compared with other algorithms can be obviously

Table 9
Best model parameters obtained by MSFS for Multi-crystalline S75 PV module under different environmental conditions.

	Parameter	1000 W/m^2 25 °C	800 W/m^2 25 °C	600 W/m^2 25 °C	400 W/m^2 25 °C	200 W/m^2 25 °C	1000 W/m^2 50 °C	1000 W/m^2 60 °C
SDM	I_{ph} (A)	4.696724	3.765089	2.824748	1.884411	0.944105	4.740179	4.764275
	I_{sd} (μA)	0.024178	0.000351	0.000353	0.006031	0.025235	1.000000	1.000000
	R_s (Ω)	0.007214	0.010986	0.011406	0.007412	0.007328	0.008003	0.009237
	R_{sh} (Ω)	10.366314	7.934447	8.876908	9.651382	11.431687	16.360680	10.903464
	n	1.221903	1.000000	1.000000	1.137500	1.234222	1.285144	1.202068
	RMSE	0.025321	0.017511	0.022756	0.009334	0.001592	0.028732	0.038277
DDM	I_{ph} (A)	4.696724	3.765089	2.824749	1.884401	0.944105	4.732801	4.755892
	I_{sd1} (μA)	0.000000	0.000351	0.000353	0.999891	0.025235	1.000000	1.000000
	R_s (Ω)	0.007214	0.010986	0.011406	0.007417	0.007328	0.007487	0.008752
	R_{sh} (Ω)	10.366317	7.934456	8.876842	9.662220	11.431687	70.954598	25.874623
	n_1	3.040947	1.000000	1.000000	3.994840	1.234222	1.345305	1.258310
	I_{sd2} (μA)	0.024178	0.000000	0.000000	0.005998	0.000000	1.000000	1.000000
	n_2	1.221903	3.727625	3.805885	1.137186	3.267232	1.345305	1.258310
	RMSE	0.025321	0.017511	0.022756	0.009334	0.001592	0.026085	0.034588

Table 10
Best model parameters obtained by MSFS for Mono-crystalline SM55 PV module under different environmental conditions.

	Parameter	1000 W/m^2 25 °C	800 W/m^2 25 °C	600 W/m^2 25 °C	400 W/m^2 25 °C	200 W/m^2 25 °C	1000 W/m^2 50 °C	1000 W/m^2 60 °C
SDM	I_{ph} (A)	3.412021	2.728411	2.047474	1.358516	0.694545	3.415757	3.440979
	I_{sd} (μA)	0.000212	0.000213	0.009065	0.085486	0.001673	0.017377	0.386126
	R_s (Ω)	0.014209	0.015575	0.012210	0.007505	0.019321	0.013396	0.013024
	R_{sh} (Ω)	8.761742	10.022704	13.147554	29.342426	7.867905	17.382072	30.935897
	n	1.000000	1.000000	1.190043	1.349415	1.087582	1.112773	1.155464
	RMSE	0.012147	0.024563	0.011178	0.006053	0.002499	0.010802	0.009833
DDM	I_{ph} (A)	3.410079	2.725874	2.047044	1.358432	0.694546	3.412777	3.440535
	I_{sd1} (μA)	0.000239	0.000250	0.006463	0.027138	0.001682	0.004906	0.121121
	R_s (Ω)	0.014160	0.015474	0.012361	0.008380	0.019297	0.013629	0.013207
	R_{sh} (Ω)	9.378986	10.917232	13.721929	31.297710	7.867199	25.255084	35.279279
	n_1	1.005210	1.006924	1.170543	1.269842	1.087876	1.048902	1.091319
	I_{sd2} (μA)	0.682765	0.621829	0.960161	0.978240	0.000589	0.997306	0.994871
	n_2	2.932073	3.438585	2.161877	1.884047	3.691893	1.668541	1.376671
	RMSE	0.012265	0.024601	0.011163	0.006002	0.002499	0.010259	0.009741

Table 11
Best model parameters obtained by MSFS for Thin-film ST40 PV module under different environmental conditions.

	Parameter	1000 W/m^2 25 °C	800 W/m^2 25 °C	600 W/m^2 25 °C	400 W/m^2 25 °C	200 W/m^2 25 °C	1000 W/m^2 50 °C	1000 W/m^2 60 °C
SDM	I_{ph} (A)	2.701906	2.167982	1.622439	1.083355	0.546079	2.744496	2.767247
	I_{sd} (μA)	0.082480	1.000000	1.000000	1.000000	1.000000	1.000000	1.000000
	R_s (Ω)	0.030721	0.026181	0.028704	0.031449	0.048553	0.028363	0.030681
	R_{sh} (Ω)	5.319522	4.633834	6.303380	7.386382	8.307333	3.477619	2.863332
	n	1.254704	1.459290	1.455639	1.451668	1.437201	1.303426	1.207672
	RMSE	0.018839	0.014542	0.012510	0.007873	0.007676	0.017495	0.019635
DDM	I_{ph} (A)	2.699657	2.163360	1.618993	1.081131	0.544652	2.737420	2.759459
	I_{sd1} (μA)	0.028760	1.000000	1.000000	1.000000	1.000000	1.000000	1.000000
	R_s (Ω)	0.030963	0.024937	0.027048	0.028871	0.043446	0.027478	0.029842
	R_{sh} (Ω)	5.707973	5.254000	7.228460	8.221486	8.978428	4.006364	3.252758
	n_1	1.190604	1.531708	1.529390	1.527586	1.516650	1.366996	1.266562
	I_{sd2} (μA)	0.999295	1.000000	1.000000	1.000000	1.000000	1.000000	1.000000
	n_2	1.714313	1.531708	1.529390	1.527585	1.516650	1.366996	1.266562
	RMSE	0.018634	0.013258	0.011097	0.006921	0.006919	0.015520	0.017964

observed. After about 3000 fitness function evaluations, the convergence curve of MSFS starts to get ahead of the convergence curves of the other algorithms. The advantage of convergence speed means that MSFS can obtain better solutions with equal computational costs.

The best model parameters obtained by each algorithm are given in Table 8, and it can also be inferred that there are many locally optimal solutions in the neighborhood of the optimal solution of this case. The consistency between the best SDM obtained by MSFS and the actual behavior of the PV module is illustrated in Fig. 8, and the detail data are given in Table A.2. Similarly with the situations of the previous two cases, it can be found that the obtained SDM is highly consistent with the experimental data thus it can be used to accurately describe the behavior of the PV module. The maximum value of IAE is 4.8328E−03.

From what have been discussed above, it can be found that the proposed MSFS is an accurate, reliable, and effectively approach for estimating the unknown SDM parameters and DDM parameters for solar cell and PV module.

4.4. SDM and DDM on different types of PV module under different environmental conditions

Due to space limitations, only the optimal model parameters obtained by MSFS for each situation are given below, as Tables 9–11. Meanwhile, the *I*–*V* characteristics of the estimated models

Table A.1
Comparison between the experimental data and the best SDM and DDM obtained by MSFS for the solar cell.

	Measured data		SDM		DDM	
Item	Voltage (V)	Current (A)	Current (A)	IAE	Current (A)	IAE
1	−0.2057	0.764	0.76408770	8.7704E−05	0.76398341	1.6587E−05
2	−0.1291	0.762	0.76266309	6.6309E−04	0.76260410	6.0410E−04
3	−0.0588	0.7605	0.76135531	8.5531E−04	0.76133770	8.3770E−04
4	0.0057	0.7605	0.76015399	3.4601E−04	0.76017379	3.2621E−04
5	0.0646	0.76	0.75905521	9.4479E−04	0.75910768	8.9232E−04
6	0.1185	0.759	0.75804235	9.5765E−04	0.75812142	8.7858E−04
7	0.1678	0.757	0.75709165	9.1654E−05	0.75718861	1.8861E−04
8	0.2132	0.757	0.75614136	8.5864E−04	0.75624361	7.5639E−04
9	0.2545	0.7555	0.75508687	4.1313E−04	0.75517730	3.2270E−04
10	0.2924	0.754	0.75366388	3.3612E−04	0.75372235	2.7765E−04
12	0.3585	0.7465	0.74735385	8.5385E−04	0.74730144	8.0144E−04
13	0.3873	0.7385	0.74011722	1.6172E−03	0.74001066	1.5107E−03
14	0.4137	0.728	0.72738223	6.1777E−04	0.72724695	7.5305E−04
15	0.4373	0.7065	0.70697265	4.7265E−04	0.70685030	3.5030E−04
16	0.459	0.6755	0.67528015	2.1985E−04	0.67521054	2.8946E−04
17	0.4784	0.632	0.63075827	1.2417E−03	0.63076076	1.2392E−03
18	0.496	0.573	0.57192836	1.0716E−03	0.57199473	1.0053E−03
19	0.5119	0.499	0.49960702	6.0702E−04	0.49970614	7.0614E−04
20	0.5265	0.413	0.41364879	6.4879E−04	0.41373367	7.3367E−04
21	0.5398	0.3165	0.31751011	1.0101E−03	0.31754620	1.0462E−03
22	0.5521	0.212	0.21215494	1.5494E−04	0.21212299	1.2299E−04
23	0.5633	0.1035	0.10225131	1.2487E−03	0.10216328	1.3367E−03
24	0.5736	−0.01	−0.00871754	1.2825E−03	−0.00879175	1.2082E−03
25	0.5833	−0.123	−0.12550741	2.5074E−03	−0.12554343	2.5434E−03
26	0.59	−0.21	−0.20847233	1.5277E−03	−0.20837159	1.6284E−03

Table A.2
Comparison between the experimental data and the best SDM obtained by MSFS for the PV module.

	Measured data		SDM	
Item	Voltage (V)	Current (A)	Current (A)	IAE
1	0.1248	1.0315	1.02911916	0.00238084
2	1.8093	1.03	1.02738107	0.00261893
3	3.3511	1.026	1.02574180	0.00025820
4	4.7622	1.022	1.02410715	0.00210715
5	6.0538	1.018	1.02229180	0.00429180
6	7.2364	1.0155	1.01993068	0.00443068
7	8.3189	1.014	1.01636311	0.00236311
8	9.3097	1.01	1.01049615	0.00049615
9	10.2163	1.0035	1.00062897	0.00287103
10	11.0449	0.988	0.98454838	0.00345162
11	11.8018	0.963	0.95952168	0.00347832
12	12.4929	0.9255	0.92283882	0.00266118
13	13.1231	0.8725	0.87259966	0.00009966
14	13.6983	0.8075	0.80727426	0.00022574
15	14.2221	0.7265	0.72833648	0.00183648
16	14.6995	0.6345	0.63713800	0.00263800
17	15.1346	0.5345	0.53621306	0.00171306
18	15.5311	0.4275	0.42951132	0.00201132
19	15.8929	0.3185	0.31877448	0.00027448
20	16.2229	0.2085	0.20738951	0.00111049
21	16.5241	0.101	0.09616717	0.00483283
22	16.7987	−0.008	−0.00832539	0.00032539
23	17.0499	−0.111	−0.11093648	0.00006352
24	17.2793	−0.209	−0.20924727	0.00024727
25	17.4885	−0.303	−0.30086359	0.00213641

and the actual PV modules are contrastively given in Figs. 9–14. From these tables and figures, it can be observed that for different types of PV modules under different environmental conditions, MSFS can obtain sufficiently accurate models and the RMSE values corresponding to the achieved models are of the order of 10^{-2} or 10^{-3}. This shows that MSFS has good practicability.

5. Conclusions

In this study, a modified stochastic fractal search algorithm, MSFS, is proposed for effectively estimating the unknown SDM parameters and DDM parameters of solar cells and PV modules. Different with the basic stochastic fractal search algorithm, the proposed algorithm employs a different diffusion process, simplified update processes, and a population size reduction strategy. By comprehensively testing on three benchmark estimation cases and three different types of PV modules under different irradiances and temperatures, the proposed strategy is proved to be effective and practical. Meanwhile, compared with seven recently published algorithms which are designed for the parameter estimation of solar cells and PV modules, i.e. IJAYA, PGJAYA, MLBSA, PSFS, TLABC, PSOCS, and DSCSE, MSFS shows its advantages in the aspects of accuracy, convergence speed, and stability.

Future work can be focused on incorporating the MSFS into the simulation and control of PV systems such as maximum power point tracking, fault detection, and so on. Meanwhile, considering its universality, exploring its availability for other complex practical optimization problems would be another focus of future work.

CRediT authorship contribution statement

Shuhui Xu: Writing – original draft, Writing – review & editing, Software, Visualization, Investigation. **Huadong Qiu:** Conceptualization, Methodology, Formal analysis, Investigation.

Declaration of competing interest

The authors declare that they have no known competing financial interests or personal relationships that could have appeared to influence the work reported in this paper.

Acknowledgments

The authors sincerely appreciate the supports provided by the National Natural Science Foundation of China (Grant No. 51905284), and sincerely thank Dr. Xu Chen for his sharing of the codes of TLABC and PSFS, Dr. Kunjie Yu for his sharing of the codes of IJAYA, PGJAYA, and MLBSA, and Prof. Huiling Chen for his sharing the code of PSOCS, and sincerely thank the anonymous reviewers for their valuable comments.

Appendix

See Tables A.1 and A.2.

References

Abbassi, A., Abbassi, R., Heidari, A.A., Oliva, D., Chen, H., Habib, A., Jemli, M., Wang, M., 2020. Parameters identification of photovoltaic cell models using enhanced exploratory salp chains-based approach. Energy 198, 117333.

Ahmad, L., Khordehgah, N., Malinauskaite, J., Jouhara, H., 2020. Recent advances and applications of solar photovoltaics and thermal technologies. Energy 207, 118254.

Ahmadianfar, I., Gong, W., Heidari, A.A., Golilarz, N.A., Samadi-Koucheksaraee, A., Chen, H., 2021. Gradient-based optimization with ranking mechanisms for parameter identification of photovoltaic systems. Energy Rep. 7, 3979–3997.

Ben Messaoud, R., 2020. Extraction of uncertain parameters of single-diode model of a photovoltaic panel using simulated annealing optimization. Energy Rep. 6, 350–357.

Brest, J., Maučec, M.S., 2011. Self-adaptive differential evolution algorithm using population size reduction and three strategies. Soft Comput. 15 (11), 2157–2174.

Brest, J., Maučec, M.S., Bošković, B., 2017. Single objective real-parameter optimization: Algorithm jSO. In: 2017 IEEE Congress on Evolutionary Computation. CEC, pp. 1311–1318.

Brest, J., Sepesy Maučec, M., 2008. Population size reduction for the differential evolution algorithm. Appl. Intell. 29 (3), 228–247.

Chander, S., Purohit, A., Sharma, A., Arvind, Nehra, S.P., Dhaka, M.S., 2015. A study on photovoltaic parameters of mono-crystalline silicon solar cell with cell temperature. Energy Rep. 1, 104–109.

Chen, X., Xu, B., Mei, C., Ding, Y., Li, K., 2018. Teaching–learning–based artificial bee colony for solar photovoltaic parameter estimation. Appl. Energy 212, 1578–1588.

Chen, X., Yue, H., Yu, K., 2019. Perturbed stochastic fractal search for solar PV parameter estimation. Energy 189, 116247.

Chu, W., Gao, X., Sorooshian, S., 2011. Handling boundary constraints for particle swarm optimization in high-dimensional search space. Inform. Sci. 181 (20), 4569–4581.

Easwarakhanthan, T., Bottin, J., Bouhouch, I., Boutrit, C., 1986. Nonlinear minimization algorithm for determining the solar cell parameters with microcomputers. Int. J. Sol. Energy 4 (1), 1–12.

Ebrahimi, S.M., Salahshour, E., Malekzadeh, M., Francisco, G., 2019. Parameters identification of PV solar cells and modules using flexible particle swarm optimization algorithm. Energy 179, 358–372.

Fan, Y., Wang, P., Heidari, A.A., Chen, H., Turabieh, Hamza, Mafarja, M., 2022. Random reselection particle swarm optimization for optimal design of solar photovoltaic modules. Energy 239, 121865.

Fan, Y., Wang, P., Heidari, A.A., Zhao, X., Turabieh, H., Chen, H., 2021. Delayed dynamic step shuffling frog-leaping algorithm for optimal design of photovoltaic models. Energy Rep. 7, 228–246.

Fernandes, C.M., Fachada, N., Laredo, J.L.J., Merelo, J.J., Rosa, A.C., 2020. Population sizing of cellular evolutionary algorithms. Swarm Evol. Comput. 58, 100721.

Gandomi, A.H., Yang, X.-S., 2012. Evolutionary boundary constraint handling scheme. Neural Comput. Appl. 21 (6), 1449–1462.

Hu, Z., Gong, W., Li, S., 2021. Reinforcement learning-based differential evolution for parameters extraction of photovoltaic models. Energy Rep. 7, 916–928.

Jiao, S., Chong, G., Huang, C., Hu, H., Wang, M., Heidari, A.A., Chen, H., Zhao, X., 2020. Orthogonally adapted Harris hawks optimization for parameter estimation of photovoltaic models. Energy 203, 117804.

Jordehi, A.R., 2016. Parameter estimation of solar photovoltaic (PV) cells: A review. Renew. Sustain. Energy Rev. 61, 354–371.

Kabir, E., Kumar, P., Kumar, S., Adelodun, A.A., Kim, K.-H., 2018. Solar energy: Potential and future prospects. Renew. Sustain. Energy Rev. 82, 894–900.

Kennedy, J., 2003. Bare bones particle swarms. In: Proceedings of the 2003 IEEE Swarm Intelligence Symposium. SIS'03 (Cat. No. 03EX706), pp. 80–87.

Kler, D., Goswami, Y., Rana, K.P.S., Kumar, V., 2019. A novel approach to parameter estimation of photovoltaic systems using hybridized optimizer. Energy Convers. Manage. 187, 486–511.

Kler, D., Sharma, P., Banerjee, A., Rana, K.P.S., Kumar, V., 2017. PV cell and module efficient parameters estimation using evaporation rate based water cycle algorithm. Swarm Evol. Comput. 35, 93–110.

Liang, J., Qiao, K., Yu, K., Ge, S., Qu, B., Xu, R., Li, K., 2020. Parameters estimation of solar photovoltaic models via a self-adaptive ensemble-based differential evolution. Sol. Energy 207, 336–346.

Liu, Y., Heidari, A.A., Ye, X., Chi, C., Zhao, X., Ma, C., Turabieh, H., Chen, H., Le, R., 2021a. Evolutionary shuffled frog leaping with memory pool for parameter optimization. Energy Rep. 7, 584–606.

Liu, Y., Heidari, A.A., Ye, X., Liang, G., He, C., 2021b. Boosting slime mould algorithm for parameter identification of photovoltaic models. Energy (5), 121164.

Merchaoui, M., Sakly, A., Mimouni, M.F., 2018. Particle swarm optimisation with adaptive mutation strategy for photovoltaic solar cell/module parameter extraction. Energy Convers. Manage. 175, 151–163.

Mi, X., Liao, Z., Li, S., Gu, Q., 2021. Adaptive teaching–learning-based optimization with experience learning to identify photovoltaic cell parameters. Energy Rep. 7, 4114–4125.

Mohamed, H., Ben Jebli, M., Ben Youssef, S., 2019. Renewable and fossil energy, terrorism, economic growth, and trade: Evidence from France. Renew. Energy 139, 459–467.

Muangkote, N., Sunat, K., Chiewchanwattana, S., Kaiwinit, S., 2019. An advanced onlooker-ranking-based adaptive differential evolution to extract the parameters of solar cell models. Renew. Energy 134, 1129–1147.

Naeijian, M., Rahimnejad, A., Ebrahimi, S.M., Pourmousa, N., Gadsden, S.A., 2021. Parameter estimation of PV solar cells and modules using Whippy Harris Hawks Optimization Algorithm. Energy Rep. 7, 4047–4063.

Pan, F., Xiaohui, H., Eberhart, R., Yaobin, C., 2008. An analysis of Bare Bones Particle Swarm. In: 2008 IEEE Swarm Intelligence Symposium. pp. 1–5.

Piotrowski, A.P., Napiorkowski, J.J., Piotrowska, A.E., 2020. Population size in particle swarm optimization. Swarm Evol. Comput. 58, 100718.

Poláková, R., Tvrdík, J., Bujok, P., 2019. Differential evolution with adaptive mechanism of population size according to current population diversity. Swarm Evol. Comput. 50, 100519.

Ridha, H.M., Hizam, H., Gomes, C., Heidari, A.A., Chen, H., Ahmadipour, M., Muhsen, D.H., Alghrairi, M., 2021. Parameters extraction of three diode photovoltaic models using boosted LSHADE algorithm and Newton Raphson method. Energy 224, 120136.

Salimi, H., 2015. Stochastic fractal search: A powerful metaheuristic algorithm. Knowl.-Based Syst. 75, 1–18.

Sansaniwal, S.K., Sharma, V., Mathur, J., 2018. Energy and exergy analyses of various typical solar energy applications: A comprehensive review. Renew. Sustain. Energy Rev. 82, 1576–1601.

Taghezouit, B., Harrou, F., Sun, Y., Arab, A.H., Larbes, C., 2021. A simple and effective detection strategy using double exponential scheme for photovoltaic systems monitoring. Sol. Energy 214, 337–354.

Tanabe, R., Fukunaga, A.S., 2014. Improving the search performance of SHADE using linear population size reduction. In: 2014 IEEE Congress on Evolutionary Computation. CEC, pp. 1658–1665.

Wang, K., He, Y., Kan, A., Yu, W., Wang, D., Zhang, L., Zhu, G., Xie, H., She, X., 2019. Significant photothermal conversion enhancement of nanofluids induced by Rayleigh-Bénard convection for direct absorption solar collectors. Appl. Energy 254, 113706.

Wang, J., Yang, B., Li, D., Zeng, C., Chen, Y., Guo, Z., Zhang, X., Tan, T., Shu, H., Yu, T., 2021a. Photovoltaic cell parameter estimation based on improved equilibrium optimizer algorithm. Energy Convers. Manage. 236, 114051.

Wang, M., Zhang, Q., Chen, H., Heidari, A.A., Mafarja, M., Turabieh, H., 2021b. Evaluation of constraint in photovoltaic cells using ensemble multi-strategy shuffled frog leading algorithms. Energy Convers. Manage. 244, 114484.

Weng, X., Heidari, A.A., Liang, G., Chen, H., Ma, X., Mafarja, M., Turabieh, H., 2021. Laplacian Nelder–Mead spherical evolution for parameter estimation of photovoltaic models. Energy Convers. Manage. 243, 114223.

Xiong, G., Li, L., Mohamed, A.W., Yuan, X., Zhang, J., 2021. A new method for parameter extraction of solar photovoltaic models using gaining–sharing knowledge based algorithm. Energy Rep. 7, 3286–3301.

Xiong, G., Zhang, J., Yuan, X., Shi, D., He, Y., Yao, G., 2018. Parameter extraction of solar photovoltaic models by means of a hybrid differential evolution with whale optimization algorithm. Sol. Energy 176, 742–761.

Xu, S., Wang, Y., 2017. Parameter estimation of photovoltaic modules using a hybrid flower pollination algorithm. Energy Convers. Manage. 144, 53–68.

Yang, B., Wang, J., Zhang, X., Yu, T., Yao, W., Shu, H., Zeng, F., Sun, L., 2020. Comprehensive overview of meta-heuristic algorithm applications on PV cell parameter identification. Energy Convers. Manage. 208, 112595.

Yu, K., Liang, J.J., Qu, B.Y., Chen, X., Wang, H., 2017. Parameters identification of photovoltaic models using an improved JAYA optimization algorithm. Energy Convers. Manage. 150, 742–753.

Yu, K., Liang, J.J., Qu, B.Y., Cheng, Z., Wang, H., 2018. Multiple learning backtracking search algorithm for estimating parameters of photovoltaic models. Appl. Energy 226, 408–422.

Yu, K., Qu, B., Yue, C., Ge, S., Chen, X., Liang, J., 2019. A performance-guided JAYA algorithm for parameters identification of photovoltaic cell and module. Appl. Energy 237, 241–257.

Zhang, Y., Ma, M., Jin, Z., 2020a. Backtracking search algorithm with competitive learning for identification of unknown parameters of photovoltaic systems. Expert Syst. Appl. 160, 113750.

Zhang, Y., Ma, M., Jin, Z., 2020b. Comprehensive learning Jaya algorithm for parameter extraction of photovoltaic models. Energy 211, 118644.

Zhou, W., Wang, P., Heidari, A.A., Zhao, X., Turabieh, H., Mafarja, M., Chen, H., 2021. Metaphor-free dynamic spherical evolution for parameter estimation of photovoltaic modules. Energy Rep. 7, 5175–5202.